Bioorganic & Medicinal Chemistry 22 (2014) 366–373

Contents lists available at ScienceDirect

Bioorganic & Medicinal Chemistry

journal homepage: www.elsevier.com/locate/bmc

Design, synthesis and evaluation of novel indole derivatives as AKT inhibitors

Dezhi Yang, Peng Wang, Jianzhen Liu, Hualu Xing, Yang Liu, Wencheng Xie, Guisen Zhao *

Department of Medicinal Chemistry, Key Laboratory of Chemical Biology (Ministry of Education), School of Pharmaceutical Sciences, Shandong University, Jinan, Shandong 250012, PR China

ARTICLE INFO

Article history:
Received 28 August 2013
Revised 7 November 2013
Accepted 8 November 2013
Available online 17 November 2013

Keywords:
AKT inhibitors
GSK3β
Inhibition rate
Tetra-substituted indoles

ABSTRACT

Herein, we describe the discovery and synthesis of a new series of 1,2,4,7-tetra-substituted indole derivatives as novel AKT inhibitors by optimization of a weak hit methyl 4-(2-aminoethoxy)-1*H*-indole-2-carboxylate (**1**). Both representative compounds **6a** and **6o** exhibited the most potent inhibitory activities against AKT1, with inhibition rates of 72.5% and 78.6%, respectively, at concentrations of 10 nM. In addition, compounds **6a** and **6o** also potently inhibited the phosphorylation of the downstream GSK3 protein and displayed slightly better anti-proliferative activities in a prostate cancer cell line.

1. Introduction

The serine/threonine kinase AKT, also known as protein kinase B (PKB), plays a key role in the regulation of cell survival, proliferation and growth.[1] PKB has three isoforms (i.e., AKT1, AKT2, and AKT3), which have approximately 90% sequence identity in the kinase domain and 97–100% sequence identity in the ATP-binding site.[2] The three highly homologous isoforms of AKT are transcribed from independent genes and have overlapping but distinct functions.[3] AKT1 mediates signals downstream of phosphatidylinositol 3-kinase (PI3K) activation, which promotes cell survival and proliferation. AKT2 activation is associated with insulin-mediated metabolic processes. AKT3$^{-/-}$ mice have reduced brain size and weight, which might be attributed to reduced cell size and cell number. The net result of the activation of all of the AKT isoforms is the prevention of apoptosis and promotion of cell proliferation, which favors tumorigenesis.[3] AKT belongs to the PI3K–AKT signaling pathway, and the unregulated activation of this pathway is a crucial feature in many cancers.[4] AKT is over-expressed or activated persistently in many cancers, such as ovarian, breast and pancreatic cancers.[5,6] Activated AKT phosphorylates a series of substrates, such as glycogen synthase kinase 3 (GSK-3), pro-apoptotic protein Bad, apoptosis signal-regulating kinase 1 (ASK-1) and caspase-9, which could block the apoptosis pathway, promote cell proliferation, and maintain the survival of tumor cells.[7,8] Phosphorylation by AKT leads to the loss of the proapoptotic properties of Bad, which is a member of the Bcl-2 apoptosis-regulating proteins.[9] ASK-1 is a positive regulator of cell apoptosis by activating p38 and Jun amino-terminal kinases (JNKs).[10] AKT can phosphorylate ASK1 on Ser83 and inactivates the apoptotic function of ASK1, leading to the enhancement of cell survival.[11] Caspase-9 is an important protease in the intrinsic apoptotic pathway.[12] AKT inhibits its pro-apoptotic activity via phosphorylation on Ser196.[13,14] Cyclin-dependent kinase inhibitors, such as p21 and p27, terminate the cell cycle, but once phosphorylated by AKT, p21 and p27 lose the anti-cell cycle function.[15,16] AKT-dependent phosphorylation of GSK3 (GSK3α and GSK3β) is likely to drive cell proliferation by controlling the stability and synthesis of the proteins involved in cell-cycle entry. The GSK3-mediated the phosphorylation of the G1 cyclins, cyclin D and cyclin E, and the transcription factors *c-jun* and *c-myc* play a central role in the G1-to-S-phase cell-cycle transition, targeting them for proteasomal degradation.[17–20] Therefore, AKT has been suggested as one of the most attractive targets for new anticancer drug development.

Herein, we describe the optimization of lead compound **1** (Fig. 1), which was discovered via a random screening of a self-established focused library and structure based drug design. Originally, compound **1** exhibited inhibitory activity against AKT1 with an inhibition rate of 48.6% at a concentration of 10 nM. Molecular modeling of compound **1** with AKT1 (Fig. 2) indicated that the amino group of the compound formed two hydrogen bonds with residues Glu234 and Glu278 in the B pocket of AKT1, the methyl ester group at position 2 of lead 1 entered into pocket A, and pocket C of AKT1 was unoccupied. We hypothesized that the inhibitory activities of AKT1 could be improved either by increasing the affinity of

* Corresponding author. Tel./fax: +86 531 88382009.
E-mail address: guisenzhao@sdu.edu.cn (G. Zhao).

0968-0896/$ - see front matter © 2013 Elsevier Ltd. All rights reserved.
http://dx.doi.org/10.1016/j.bmc.2013.11.022

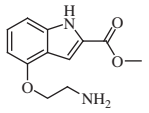

1

Figure 1. Structure of compound **1**.

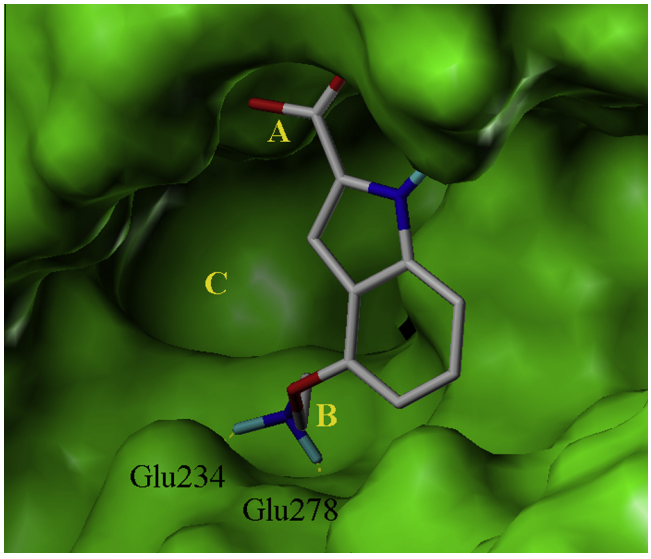

Figure 2. Molecular docking mode of lead **1** with the AKT1 crystal structure (PDB: 4GV1).

compounds for pocket A and/or B or by occupying pocket C. Therefore, we replaced methyl ester at position 2 in compound **1** with its bioisostere oxadiazole ring, we introduced a substituent group on the α-carbon of the amino group on the side chain at the C-4 position, and we introduced methoxy, bromine or chlorine at the C-7 position to design a series of indole derivatives and evaluate their inhibitory activities against AKT1.

2. Results and discussion

2.1. Chemistry

The synthesis of the indole derivatives is depicted in Scheme 1. Intermediate **2** was obtained in previous studies.[21] Intermediate **3** was obtained by removal of the benzyl group of compound **2** using palladium on carbon or *N*,*N*-dimethylaniline. Intermediates **4** were chiral amino acids and commercially available. Compound **4** reacted with thionyl chloride in the presence of methanol to produce their methyl esters, which were treated with di-*tert*-butyl dicarbonate affording the desired *t*-butyloxy carbonyl protection of the amino esters, which were reduced with lithium aluminum hydride yielding chiral alcohol **5**.[22] Compounds **6** were produced by coupling **3** with chiral alcohol **5** via a Mitsunobu reaction[23] followed by removal of the *t*-butyloxy carbonyl.

2.2. Bioassays and structure–activity relationships

The kinase inhibitory activities against AKT1 and the antiproliferative activities of the target compounds were evaluated in vitro in the PC-3 cell line, and GSK690693,[24] which is an AKT inhibitor, was used as the positive control (Table 1).

As shown in Table 1, most compounds exhibited moderate inhibitory activities against AKT1 compared to the reference, GSK690693. The spatial configuration (R or S) of the compounds exhibited irregular inhibitory activities against AKT1 (**6a** vs **6b** and **6f** vs **6g**). Compounds with hydrophobic aromatic rings on the side chain exhibited more potent inhibitory activities compared to those with hydrophobic aliphatic groups (**6a** vs **6c**, **6o** vs **6s**), which indicated that the hydrophobic aromatic rings most likely interacted with the glycine rich loop (G-loop) of AKT1 to generate hydrophobic interactions. In addition, the methyl ester group in compound **6b** was replaced by the oxadiazole moiety (bioisosteristere) resulting in compound **6o**, which exhibited the most potent inhibitory activities. In addition, compounds **6a**, **6h**, **6l** and **6o** exhibited higher potency against AKT1 than hit **1**, which demonstrated that modification of lead **1** increased the potency.

The molecular docking of compound **6a** with the crystal structure of AKT1 (PDB: 4GV1) indicated that **6a** was nicely bound to the ATP cleft of AKT1 via hydrogen bonds that were formed between the amino group and the carboxylic acid side chains of Glu234 and Glu278 in pocket B. The benzyl group on the α-carbon of the amino group on the side chain at the C-4 position entered into the back of pocket C, as hypothesized, and the methyl ester entered into pocket A. In addition, the methoxy group at the C-7 position stretched into another pocket on the left side of pocket B, which increased

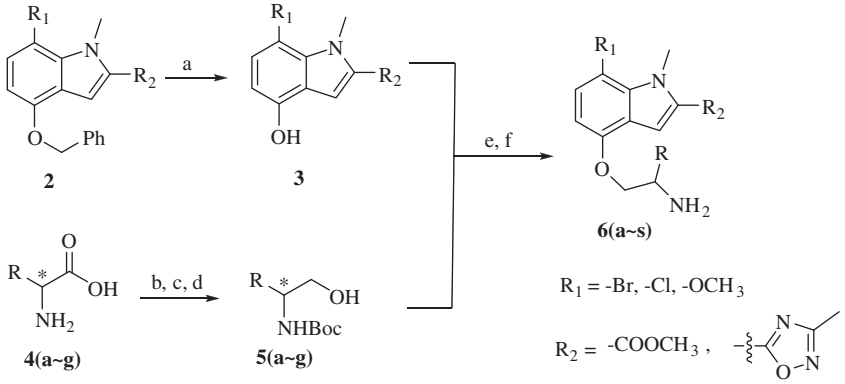

4a: L-Phenylalanine; **4b**: D-Phenylalanine; **4c**:L-Tryptophan; 4**d**: D-Tryptophan; **4e**: L-Leucine; **4f**: L-Methionine; **4g**: L-Isoleucine

Scheme 1. Reagents and conditions: (a) 10% Pd/C, CH_3OH/THF, H_2, rt or $AlCl_3$, *N*,*N*-dimethylaniline, CH_2Cl_2, 0–25 °C, 1 h; (b) $SOCl_2$, CH_3OH, 0–25 °C, overnight; (c) Boc_2O, Et_3N, CH_2Cl_2, 0 °C to rt, overnight; (d) THF, $LiAlH_4$, 0–25 °C, 4 h; (e) PPh_3, DIAD, THF, 0–25 °C, 12 h; (f) HCl/ethyl acetate, 1 h, rt.

Table 1
The inhibitory effects of indole derivatives on AKT1 activity and on PC-3 cell growth

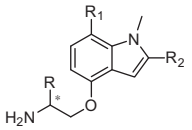

Code	R	R^1	R^2	*R*/*S*	Inhibition of AKT1 activity[a] (%)	IC_{50} (μM) for inhibiting PC-3 cell growth[b]
6a		OCH_3	$COOCH_3$	*S*	72.5	3.8 ± 0.1
6b		OCH_3	$COOCH_3$	*R*	38.9	16.1 ± 3.6
6c	$CH_2CH(CH_3)_2$	OCH_3	$COOCH_3$	*S*	27.8	7.8 ± 0.3
6d	$CH_2CH_2SCH_3$	OCH_3	$COOCH_3$	*S*	7.7	7.0 ± 0.5
6e		OCH_3	$COOCH_3$	*S*	48.7	11.3 ± 0.3
6f		Br	$COOCH_3$	*S*	56.1	6.0 ± 0.1
6g		Br	$COOCH_3$	*R*	55.4	9.7 ± 1.1
6h	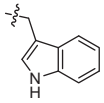	Br	$COOCH_3$	*S*	73.0	5.0 ± 0.1
6i	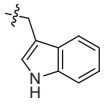	Br	$COOCH_3$	*R*	36.0	4.9 ± 0.1
6j		Cl	$COOCH_3$	*S*	34.2	7.6 ± 0.6
6k		Cl	$COOCH_3$	*R*	60.3	4.8 ± 0.3
6l	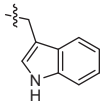	Cl	$COOCH_3$	*S*	73.5	3.2 ± 0.4
6m	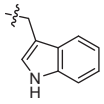	Cl	$COOCH_3$	*R*	58.4	5.5 ± 0.2
6n		OCH_3		*S*	55.7	5.1 ± 0.1
6o		OCH_3		*R*	78.6	5.3 ± 0.4
6p	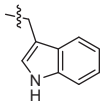	OCH_3		*S*	43.3	5.7 ± 0.4
6q	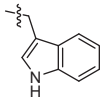	OCH_3		*R*	56.7	2.8 ± 0.1
6r	$CH_2CH_2SCH_3$	OCH_3		*S*	55.5	9.1 ± 0.7
6s	$CH_2CH(CH_3)_2$	OCH_3		*S*	42.0	11.4 ± 1.4
1	—	—	—	—	48.6	5.9 ± 0.6
GSK690693	—	—	—	—	58.3	15.5 ± 0.4

[a] The inhibition rates of AKT1 activity were determined at 10 nM concentrations of the tested compounds. The data shown are the mean of three independent experiments.
[b] IC_{50} indicates the concentration of the tested compound that inhibits 50% of PC-3 cell growth.

the binding of AKT1 for **6a** compared to lead **1**, as shown in Figure 3.

The kinase inhibitory activities of selected compounds **6a** and **6o** were further investigated by western blot analysis. The results (Fig. 4) demonstrated that the two compounds dose-dependently inhibited the phosphorylation of GSK3β, a downstream substrate of AKT, which was in agreement with the reported selective AKT inhibitors.[25,26]

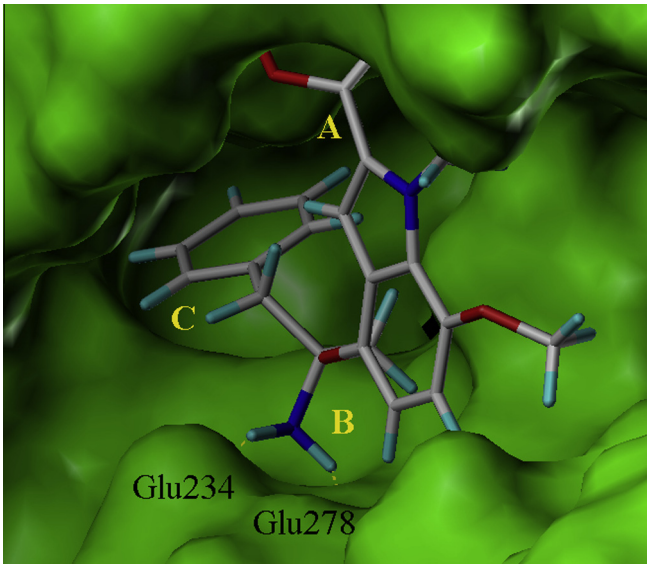

Figure 3. Molecular docking mode of **6a** with the AKT1 crystal structure (PDB: 4GV1).

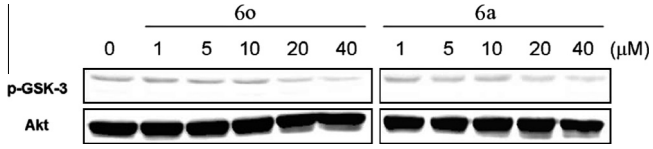

Figure 4. Compounds **6a** and **6o** dose-dependently inhibited the phosphorylation of GSK3 in the PC-3 cells.

2.3. Conclusion

In conclusion, a new series of 1,2,4,7-tetra-substituted indole derivatives were synthesized and evaluated as AKT inhibitors. Among these compounds, compounds **6a** and **6o** exhibited the most potent inhibitory activities against AKT1 with inhibition rates of 72.5% and 78.6%, respectively, and antiproliferative activities on the human prostate cancer cell line (PC-3) with IC_{50} values of 3.8 and 5.3 μM, respectively. The AKT1 inhibition of compounds **6a** and **6o** were further confirmed via cell lysate assays. These types of compounds may serve as leads for further optimization of novel AKT inhibitors.

3. Experimental

All of the materials were obtained from commercial suppliers and used without further purification. All of the reactions were monitored by thin layer chromatography (TLC), and silica gel plates with fluorescence F_{254} were used and visualized with UV light. All of the products were characterized by NMR. All of the ^1H NMR spectra were recorded on a Bruker advance DPX600 model Spectrometer in DMSO-d_6, and the chemical shifts are reported in ppm (δ). The mass spectra (MS) were measured with an API 4000. All of the melting points were determined in a Büchi capillary melting point apparatus and are uncorrected. Column chromatography was performed with silica gel using the solvents indicated.

3.1. MTT assay

The antiproliferation of the target compounds in the PC-3 cells was tested using the MTT assay. The cells were seeded into 96-well culture plates at a density of 5×10^3 cells per well and cultured in an atmosphere of 5% CO_2 at 37 °C with 100 μL/well RPMI1640 (Gibco) medium. On the second day, the cells were treated with various concentrations of the tested compounds and DMSO (black control) followed by incubation for 72 h. 5 mg/mL of the MTT (Sigma) solution was added to each well, and the cells were incubated for 4 h. The formazan crystal was extracted by DMSO for 15 min. The optical density ($OD_{570\ nm}$) was measured by a plate microreader (Bio-Rad 680). Cell growth inhibition was calculated as the ratio of the absorbance of the sample to that of the control.

3.2. In vitro AKT1 kinase activity assay

The in vitro AKT1 kinase activity was evaluated via a nonradioactive assay using the AKT kinase kit (9840s) (CST) and pan-AKT antibody (CST). Briefly, PC-3 cells were treated with DMSO (the black control) or 10 nM concentrations of the tested compounds for 1 h. 80 μL of lysate was prepared for each tested well, and 20 μL of this lysate was used to detect the total amount of AKT. In addition, the remaining 60 μL was used to immune precipitate phosphor-AKT using immobilized antiphospho-AKT1 antibodies by overnight incubation at 4 °C. The kinase assay was performed according to the manufacturer's instructions using the GSK-3β fusion protein (CST) as a substrate. The kinase reaction was terminated with sodium dodecyl sulfate (SDS) loading buffer. Then, the samples were run on a 4–12% SDS–polyacrylamide gel electrophoresis (SDS–PAGE) gel, and the phosphorylation of GSK-3β was measured by Western blot analysis with antiphospho-GSK-3α/β (Ser21/9) antibodies. The results were detected by Bio-Rad and were quantified with Image Lab software. Lysates from the beginning were run on a 4–12% SDS–PAGE gel, and the total AKT was detected using the pan-AKT antibody. The inhibition rate of each compound was calculated using Eq. 1.

$$\text{Inhibition rate} = \frac{FI_{gsk-3(sample)}/FI_{Akt(sample)}}{FI_{gsk-3(DMSO)}/FI_{Akt(DMSO)}} \times 100\%. \quad (1)$$

$FI_{gsk\text{-}3(sample)}$ was the fluorescence intensity of the phospho-GSK-3α/β (Ser21/9) band of the tested compounds; $FI_{gsk\text{-}3(DMSO)}$ was the fluorescence intensity of the phospho-GSK-3α/β (Ser21/9) band of the blank control; $FI_{Akt(sample)}$ was the fluorescence intensity of the pan-Akt band of the tested compounds; $FI_{Akt(DMSO)}$ was the fluorescence intensity of the pan-Akt band of the blank control.

3.3. Western blot assay

Cells were seeded into 6-well culture plates at a density of 5×10^3 cells per well and cultured for 12 h. Then, the cells were collected and washed with PBS (Sigma) and 500 μL of a kinase buffer (CST), treated with various concentrations of compounds and incubated for 4 h. 80 μL of lysate was treated to obtain the supernatant. The concentration of the protein was determined through Coomassie blue staining. The proteins was run across SDS–PAGE and transferred to PVDF membranes. After blocking, the antiphospho-GSK-3α/β (Ser21/9) antibodies (CST) were added to the membranes and incubated for 12 h. Next, anti-rabbit IgG (CST) was added followed by incubation for 1 h. Finally, the results were detected using chemiluminescence and Bio-Rad.

3.4. Molecular docking

Molecular docking was performed with the Sybyl 1.1 program and the AKT1 crystal structure, which was retrieved from the Protein Data Bank (PDB: 4GV1). Protein preparation was performed by removing water molecules, and based on the ionization, hydrogen atoms were added. The structures of target compounds were treated with Chembiooffice (2010) and generated with the ligand

module by minimizing the molecule. The best one as ranked by C Score among the top 20 binding poses was chosen as the preliminary model for the subsequent minimization. The energy minimization was computed by minimizing the model in Sybyl 1.1 using the Powell method. The Tripos force field was used, and the maximum number of iterations was set to 10,000. The gradient was set to 0.05 kcal/mol. All of the target compounds were docked into AKT1 and formed hydrogen bonds and hydrophobic interactions in the model. To improve visibility, residues Glu 441 and Phe 442 and substructure GLO505 were removed, and hydrogen bonds are shown by the dotted yellow line.

3.5. General synthesis of compounds

3.5.1. General method for preparation of compounds (3a–3c)

To a solution of **2** (2 mmol) in tetrahydrofuran (15 mL) and dried methanol (6 mL), Pd/C (0.16 g) was added under a hydrogen atmosphere, which was stirred at 35 °C for 12 h. After completion of the reaction, the reaction mixture was filtered. The solvent was evaporated under reduced pressure to afford a solid, which was purified by column chromatography with petroleum ether/ethyl acetate (6:1) to obtain **3a**–**3c**.

3.5.1.1. Methyl 4-hydroxy-7-methoxy-1-methyl-1*H*-indole-2-carboxylate (3a). White solid, yield 94%, mp 100.1–101.8 °C, ^{1}H NMR (600 MHz, DMSO-d_6): δ 9.31 (s, 1H), 7.27 (s, 1H), 6.63 (d, J = 7.8 Hz, 1H), 6.29 (d, J = 7.8 Hz, 1H), 4.24 (s, 3H), 3.82 (s, 3H), 3.81 (s, 3H).MS (ESI): m/z = 236.1 $[M+H]^+$.

3.5.1.2. Methyl 7-bromo-4-hydroxy-1-methyl-1*H*-indole-2-carboxylate (3b). White solid, yield 69%, mp 106.5–109.6 °C, ^{1}H NMR (600 MHz, DMSO-d_6): δ 10.07 (s, 1H), 7.32 (d, J = 2.4 Hz, 1H), 7.25 (dd, J = 7.8 Hz and 2.4 Hz, 1H), 6.40 (dd, J = 7.8 Hz and 2.4 Hz, 1H), 4.26 (s, 3H), 3.86 (s, 3H). MS (ESI): m/z = 283.9 $[M+H]^+$.

3.5.1.3. Methyl 7-chloro-4-hydroxy-1-methyl-1*H*-indole-2-carboxylate (3c). White solid, yield 55%, mp 101.7–103.1 °C, ^{1}H NMR (600 MHz, DMSO-d_6): δ 10.08 (s, 1H), 7.31 (d, J = 2.4 Hz, 1H), 7.26 (dd, J = 7.8 Hz and 2.4 Hz, 1H), 6.41 (dd, J = 7.8 Hz and 2.4 Hz, 1H), 4.26 (s, 3H), 3.86 (s, 3H). MS (ESI): m/z = 240.2 $[M+H]^+$.

3.5.2. Method for preparation of compound (3d)

To a solution of **2** (1.7 mmol) in dried dichloromethane (12 mL), *N*,*N*-dimethylaniline (0.83 g) and aluminum trichloride (0.92) were added at 0 °C. The mixture was reacted at room temperature for 1.5 h. After completion of the reaction, 1 mol/L hydrochloric acid (20 mL) and water (20 mL) was added to the solution followed by extraction with ethyl acetate (50 × 3 mL). The organic layer was successively washed with hydrochloric acid and saturated sodium chloride, dried with anhydrous sodium sulfate, filtered and evaporated under reduced pressure to afford a solid, which was purified by column chromatography with petroleum ether/ethyl acetate (3:1) to obtain **3d**.

3.5.2.1. 7-Methoxy-1-methyl-2-(3-methyl-1,2,4-oxadiazol-5-yl)-1*H*-indole-4-ol (3d). Green solid, yield 89%, mp 125.8–127.6 °C, ^{1}H NMR (600 MHz, DMSO-d_6): δ 9.30 (s, 1H), 7.23 (s, 1H), 6.63 (d, J = 7.8 Hz, 1H), 6.28 (d, J = 7.8 Hz, 1H), 4.24 (s, 3H), 3.82 (s, 3H), 2.46 (s, 3H). MS (ESI): m/z = 260.2 $[M+H]^+$.

3.5.3. General method for preparation of compounds (5)

To a dried methanol (50 mL) solution of **4** (3.3 g, 20 mmol), thionyl chloride (3.57 g, 30 mmol) was slowly added over 30 min at 0 °C, and then, the solution was maintained at room temperature for 18 h. The solvent was evaporated to obtain a solid in quantitative yield, which was dissolved in dichloromethane (120 mL), and triethylamine (12.1 g, 120 mL) and di-*tert*-butyl dicarbonate (9.6 g, 40 mmol) were added to the dichloromethane solution. The reaction mixture was stirred at 25 °C for 24 h. After completion of the reaction, the solution was washed with phosphoric acid (50 × 3 mL), saturated sodium bicarbonate (50 × 3 mL) and saturated sodium chloride (50 × 3 mL), dried over anhydrous sodium sulfate, filtered and evaporated under reduced pressure to afford a solid to which lithium aluminum hydride (13 mmol) in the presence of dried tetrahydrofuran (25 mL) was added at 0 °C. The reaction mixture was maintained at room temperature for 4 h, and then water was added until the lithium aluminum hydride reacted completely. Next, the solution was filtered, and the residue was washed with tetrahydrofuran (20 × 2 mL). The combined organic solvent phase was evaporated under reduced pressure to yield the crude product, which was purified using column chromatography (petroleum ether/acetone) to afford **5a**–**5g**.

3.5.3.1. (*S*)-*tert*-Butyl (1-hydroxy-3-phenylpropan-2-yl)carbamate (5a). White solid, yield 82%, mp 92–93 °C, ^{1}H NMR (600 MHz, DMSO-d_6): δ 7.15–7.27 (m, 5H), 6.58 (d, J = 8.4 Hz, 1H), 4.69 (m,1H), 3.72–3.86 (m, 1H), 3.58 (br, s, 1H), 3.24–3.32 (m, 1H), 2.80 (dd, J = 13.8 Hz and 4.2 Hz), 2.57 (t, J = 9.6 Hz, 1H), 1.31 (s, 9H). MS (ESI): m/z = 252.3 $[M+H]^+$.

3.5.3.2. (*R*)-*tert*-Butyl (1-hydroxy-3-phenylpropan-2-yl)carbamate (5b). White solid, yield 75%, mp 94–96 °C, ^{1}H NMR (600 MHz, DMSO-d_6): δ 7.14–7.28 (m, 5H), 6.57 (d, J = 8.4 Hz, 1H), 4.68 (t, J = 4.2 Hz, 1H), 3.72–3.86 (m, 1H), 3.58 (br, s, 1H), 3.24–3.32 (m, 1H), 2.80 (dd, J = 13.2 Hz and 4.2 Hz, 1H), 2.57 (t, J = 9.6 Hz, 1H), 1.31 (s, 9H). MS (ESI): m/z = 252.4 $[M+H]^+$.

3.5.3.3. (*S*)-*tert*-Butyl (1-hydroxy-3-(1*H*-indol-3-yl)propan-2-yl)carbamate (5c). White solid, yield 78%, mp 94–96 °C, ^{1}H NMR (600 MHz, DMSO-d_6): δ 10.76 (s, 1H), 7.57 (d, J = 7.8 Hz, 1H), 7.31 (d, J = 7.8 Hz, 1H), 7.08 (s, 1H), 7.04 (t, J = 7.8 Hz, 1H), 6.96 (t, J = 7.2 Hz, 1H), 6.52 (d, J = 7.8 Hz, 1H), 4.63 (br, s, 1H), 3.65 (quint, J = 6.6 Hz, 1H), 3.29–3.37 (m, 2H), 2.87 (dd, J = 14.4 Hz and 6.0 Hz, 1H), 2.71 (dd, J = 14.4 Hz and 6.0 Hz, 1H), 1.35 (s, 9H). MS (ESI): m/z = 291.3 $[M+H]^+$.

3.5.3.4. (*R*)-*tert*-Butyl (1-hydroxy-3-(1*H*-indol-3-yl)propan-2-yl)carbamate (5d). White solid, yield 69%, mp 90–92 °C, ^{1}H NMR (600 MHz, DMSO-d_6): δ 10.76 (s, 1H), 7.57 (d, J = 7.8 Hz, 1H), 7.31 (d, J = 7.8 Hz, 1H), 7.08 (s, 1H), 7.05 (t, J = 7.8 Hz, 1H), 6.96 (t, J = 7.8 Hz, 1H), 6.52 (d, J = 8.4 Hz, 1H), 4.63 (t, J = 5.4 Hz, 1H), 3.65 (q, J = 6.6 Hz, 1H), 3.34–3.38 (m, 1H), 3.29–3.32 (m, 1H), 2.88 (dd, J = 14.4 Hz and 6.0 Hz, 1H), 2.71 (dd, J = 14.4 Hz and 7.2 Hz, 1H), 1.35 (s, 9H). MS (ESI): m/z = 291.5 $[M+H]^+$.

3.5.3.5. (*S*)-*tert*-Butyl (1-hydroxy-4-methylpentan-2-yl)carbamate (5e). Colorless oil, yield 58%, ^{1}H NMR (600 MHz, DMSO-d_6): δ 6.41 (d, J = 9.0 Hz, 1H), 4.53 (t, J = 5.4 Hz, 1H), 3.41–3.46 (m, 1H), 3.26–3.29 (m, 1H), 3.14–3.18 (m, 1H), 1.37–1.98 (m, 1H), 1.37 (s, 9H), 1.16–1.28 (m, 2H), 0.83 (d, J = 6.0 Hz, 3H), 0.85 (d, J = 6.6 Hz, 3H). MS (ESI): m/z = 218.4 $[M+H]^+$.

3.5.3.6. (*S*)-*tert*-Butyl (1-hydroxy-4-(methylthio)butan-2-yl)carbamate (5f). Colorless oil, yield 55%, ^{1}H NMR (600 MHz, DMSO-d_6): δ 6.53 (d, J = 8.4 Hz, 1H), 4.62 (t, J = 6.0 Hz, 1H), 3.42–3.45 (m, 1H), 3.23–3.35 (m, 1H), 3.20–3.23 (m, 1H), 2.36–2.47 (m, 2H), 2.02 (s, 3H), 1.71–1.78 (m, 1H), 1.48–1.55 (m, 1H), 1.38 (s, 9H); MS (ESI): m/z = 236.4 $[M+H]^+$.

3.5.3.7. *tert*-Butyl ((2*S*,3*S*)-1-hydroxy-3-methylpentan-2-yl)carbamate (5g). Colorless oil, yield 64%, ^{1}H NMR (600 MHz, DMSO-d_6): δ 6.42 (d, J = 9.0 Hz, 1H), 4.41 (t, J = 5.4 Hz, 1H), 3.36–3.39 (m, 1H), 3.25–3.34 (m, 3H), 1.47–1.98 (m, 1H), 1.38 (s, 9H), 0.99–1.07 (m, 1H), 0.80–0.83 (m, 6H). MS (ESI): m/z = 218.4 $[M+H]^+$.

3.5.4. General method for preparation of compounds (6)

To diisopropyl azodiformate (DIAD) (0.41 g, 2 mmol), triphenylphosphine (0.41 g, 2 mmol) and dried tetrahydrofuran (5 mL) were slowly added. After 30 min, **5** (3 mmol) in tetrahydrofuran (5 mL) was slowly added to the solution, and then, the tetrahydrofuran (10 mL) solution of **3** (0.24 g, 1 mmol) was added to the solution over the course of 30 min under a nitrogen atmosphere at 0 °C and allowed to proceed for 12 h. After completion of the reaction, the solvent was evaporated to obtain an oil, which was extracted with ethyl acetate/petroleum ether (1:3, 4 × 10 mL). The organic phase was evaporated under reduced pressure to yield an oil, which was purified by column chromatography with petroleum ether/ethyl acetate (15:1) to obtain a solid. To the solid (0.5 mmol), ethyl acetate with saturated hydrochloric acid (15 mL) was added and reacted for 1 h. The solvent was evaporated under reduced pressure to obtain the crude product, which was recrystallized with methanol/ether to obtain **6a–6s**.

3.5.4.1. (*S*)-Methyl 4-(2-amino-3-phenylpropoxy)-7-methoxy-1-methyl-1*H*-indole-2-carboxylate hydrochloride (6a). White solid, yield 84%, mp 196.2–201.8 °C, $[\alpha]_D^{25}$ +50.0° (*c* 1, MeOH), ^{1}H NMR (600 MHz, DMSO-d_6): δ 8.38 (s, 3H), 7.61 (s, 1H), 7.32–7.34 (m, 2H), 7.26–7.28 (m, 3H), 6.66 (d, J = 8.4 Hz, 1H), 6.34 (d, J = 8.4 Hz, 1H), 4.27 (s, 3H), 4.09 (dd, J = 2.4 Hz and 10.2 Hz, 1H), 3.90 (dd, J = 5.4 Hz and 10.2 Hz, 1H), 3.86 (s, 3H), 3.84 (s, 3H), 3.82–3.85 (m, 1H), 3.13 (dd, J = 5.4 Hz and 13.2 Hz, 1H), 3.04–3.08 (m, 1H). HRMS (ESI): m/z for $C_{21}H_{25}N_2O_4$ $[M+H]^+$: calculated 369.1809, found 369.1815.

3.5.4.2. (*R*)-Methyl 4-(2-amino-3-phenylpropoxy)-7-methoxy-1-methyl-1*H*-indole-2-carboxylate hydrochloride (6b). White solid, yield 89%, mp 188.3–189.9 °C, $[\alpha]_D^{25}$ −75.0° (*c* 1, MeOH): ^{1}H NMR (600 MHz, DMSO-d_6): δ 8.44 (br, s, 3H), 7.61 (s, 1H), 7.25–7.34 (m, 5H), 6.67 (d, J = 8.4 Hz, 1H), 6.34 (d, J = 8.4 Hz, 1H), 4.27 (s, 3H), 4.10 (dd, J = 3.0 Hz and 10.2 Hz, 1H), 3.91 (dd, J = 4.8 Hz and 10.8 Hz, 1H), 3.86 (s, 3H), 3.85 (s, 3H), 3.82–3.85 (m, 1H), 3.13–3.16 (m, 1H), 3.06–3.08 (m, 1H). HRMS (ESI): m/z for $C_{21}H_{25}N_2O_4$ $[M+H]^+$: calculated 369.1809, found 369.1814.

3.5.4.3. (*S*)-Methyl 4-((2-amino-4-methylpentyl)oxy)-7-methoxy-1-methyl-1*H*-indole-2-carboxylate hydrochloride (6c). White solid, yield 90%, mp 189.1–192.0 °C, $[\alpha]_D^{25}$ +14.3° (*c* 1, MeOH), ^{1}H NMR (600 MHz, DMSO-d_6): δ 8.28 (s, 3H), 7.57 (s, 1H), 6.71 (d, J = 8.4 Hz, 1H), 6.46 (d, J = 8.4 Hz, 1H), 4.27 (s, 3H), 4.22 (dd, J = 2.4 Hz and 10.2 Hz, 1H), 4.06 (dd, J = 5.4 Hz and 10.2 Hz, 1H), 3.86 (s, 3H), 3.84 (s, 3H), 3.55–3.57 (m, 1H), 1.76–1.80 (m, 1H), 1.58–1.64 (m, 2H), 0.93 (d, J = 6.6 Hz, 3H), 0.92 (d, J = 6.6 Hz, 3H).HRMS (ESI): m/z for $C_{18}H_{27}N_2O_4$ $[M+H]^+$: calculated 335.1963, found 335.1970.

3.5.4.4. (*S*)-Methyl 4-(2-amino-4-(methylthio)butoxy)-7-methoxy-1-methyl-1*H*-indole-2-carboxylate hydrochloride (6d). White solid, yield 80%, mp 219.8–223.0 °C, $[\alpha]_D^{25}$ +13.3° (*c* 1, MeOH), ^{1}H NMR (600 MHz, DMSO-d_6): δ 8.36 (br, s, 3H), 7.56 (s, 1H), 6.72 (d, J = 8.4 Hz, 1H), 6.47 (d, J = 8.4 Hz, 1H), 4.27 (s, 3H), 4.25 (m, 1H), 4.10–4.13 (m, 1H), 3.86 (s, 3H), 3.84 (s, 3H), 3.66 (s, 1H), 2.65–2.67 (m, 2H), 2.08 (s, 3H), 2.00–2.05 (m, 2H). HRMS (ESI): m/z for $C_{17}H_{25}N_2O_4S$ $[M+H]^+$: calculated 353.1530, found 353.1534.

3.5.4.5. Methyl 4-(((2*S*,3*S*)-2-amino-3-methylpentyl)oxy)-7-methoxy-1-methyl-1*H*-indole-2-carboxylate (6e). White solid, yield 88%, mp 187.0–189.1 °C, $[\alpha]_D^{25}$ +20.0° (*c* 1, MeOH), ^{1}H NMR (600 MHz, DMSO-d_6): δ 8.31 (s, 3H), 7.56 (s, 1H), 6.71 (d, J = 8.4 Hz, 1H), 6.49 (d, J = 8.4 Hz, 1H), 4.27 (s, 3H), 4.22 (dd, J = 2.4 Hz and 10.2 Hz, 1H), 4.11–4.14 (m, 1H), 3.86 (s, 3H), 3.84 (s, 3H), 3.45 (br, s, 1H), 1.91–1.95 (m, 1H), 1.57–1.61 (m, 1H), 1.25–1.30 (m, 1H), 0.98 (d, J = 7.2 Hz, 3H), 0.92 (t, J = 7.2 Hz, 3H).HRMS (ESI): m/z for $C_{18}H_{27}N_2O_4$ $[M+H]^+$: calculated 335.1965, found 335.1970.

3.5.4.6. (*S*)-Methyl 4-(2-amino-3-phenylpropoxy)-7-bromo-1-methyl-1*H*-indole-2-carboxylate hydrochloride (6f). White solid, yield 85.6%, mp 230.3–232.5 °C, $[\alpha]_D^{25}$ +25.0° (*c* 1, MeOH), ^{1}H NMR (600 MHz, DMSO-d_6): δ 8.58 (s, 3H), 7.74 (s, 1H), 7.42 (d, J = 7.8 Hz, 1H), 7.31–7.34 (m, 2H), 7.25–7.27 (m, 3H), 6.45 (d, J = 7.8 Hz, 1H), 4.36 (s, 3H), 4.18 (d, J = 10.2 Hz, 1H), 3.97–3.99 (m, 1H), 3.88 (s, 3H), 3.85–3.87 (m, 1H), 3.18–3.20 (m, 1H), 3.04–3.08 (m, 1H). HRMS (ESI): m/z for $C_{20}H_{22}BrN_2O_3$ $[M+H]^+$: calculated 417.0808, found 417.0816.

3.5.4.7. (*R*)-Methyl 4-(2-amino-3-phenylpropoxy)-7-bromo-1-methyl-1*H*-indole-2-carboxylate hydrochloride (6g). White solid, yield 93%, mp 228.2–230.9 °C, $[\alpha]_D^{25}$ −62.5° (*c* 1, MeOH), ^{1}H NMR (600 MHz, DMSO-d_6): δ 8.68 (br, s, 3H), 7.74 (s, 1H), 7.41 (d, J = 7.8 Hz, 1H), 7.31–7.32 (m, 2H), 7.25–7.27 (m, 3H), 6.45 (d, J = 7.8 Hz, 1H), 4.36 (s, 3H), 4.19 (dd, J = 3.0 Hz and 10.8 Hz, 1H), 3.97–3.99 (m, 1H), 3.88 (s, 3H), 3.82–3.83 (m, 1H), 3.20–3.23 (m, 1H), 3.04–3.08 (m, 1H). HRMS (ESI): m/z for $C_{20}H_{22}BrN_2O_3$ $[M+H]^+$: calculated 417.0808, found 417.0816.

3.5.4.8. (*S*)-Methyl 4-(2-amino-3-(1*H*-indol-3-yl)propoxy)-7-bromo-1-methyl-1*H*-indole-2-carboxylate hydrochloride (6h). White solid, yield 85%, mp 223.9–224.8 °C, $[\alpha]_D^{25}$ +50.0° (*c* 1, MeOH), ^{1}H NMR (600 MHz, DMSO-d_6): δ 11.02 (s, 1H), 8.36 (br, s, 3H), 7.51 (s, 1H), 7.59 (d, J = 7.8 Hz, 1H), 7.41 (d, J = 8.4 Hz, 1H), 7.37 (d, J = 7.8 Hz, 1H), 7.21 (d, J = 2.4 Hz, 1H), 7.08 (t, J = 7.8 Hz, 1H), 6.96 (t, J = 7.2 Hz, 1H), 6.45 (d, J = 8.4 Hz, 1H), 4.36 (s, 3H), 4.21–4.24 (m, 1H), 4.05–4.07 (m, 1H), 3.88 (s, 3H), 3.85–3.87 (m, 1H), 3.20–3.22 (m, 1H). HRMS (ESI): m/z for $C_{22}H_{23}BrN_3O_3$ $[M+H]^+$: calculated 456.0917, found 456.0924.

3.5.4.9. (*R*)-Methyl 4-(2-amino-3-(1*H*-indol-3-yl)propoxy)-7-bromo-1-methyl-1*H*-indole-2-carboxylate hydrochloride (6i). White solid, yield 80%, mp 223.9–224.6 °C, $[\alpha]_D^{25}$ −63.6° (*c* 1, MeOH), ^{1}H NMR (600 MHz, DMSO-d_6): δ 11.3 (s, 1H), 8.46 (br, s, 3H), 7.76 (s, 1H), 7.60 (dd, J = 3.0 Hz and 7.8 Hz, 1H), 7.41 (d, J = 8.4 Hz, 1H), 7.37 (d, J = 7.8 Hz, 1H), 7.21 (d, J = 2.4 Hz, 1H), 7.08 (t, J = 7.8 Hz, 1H), 6.96 (t, J = 7.2 Hz, 1H), 6.45 (d, J = 8.4 Hz, 1H), 4.36 (s, 3H), 4.22 (dd, J = 2.4 Hz and 10.2 Hz, 1H), 4.05–4.07 (m, 1H), 3.88 (s, 3H), 3.83–3.85 (m, 1H), 3.19–3.25 (m, 1H). HRMS (ESI): m/z for $C_{22}H_{23}BrN_3O_3$ $[M+H]^+$: calculated 456.0917, found 456.0925.

3.5.4.10. (*S*)-Methyl 4-(2-amino-3-phenylpropoxy)-7-chloro-1-methyl-1*H*-indole-2-carboxylate hydrochloride (6j). White solid, yield 88%, mp 235.4–237.1 °C, $[\alpha]_D^{25}$ +33.3° (*c* 1, MeOH), ^{1}H NMR (600 MHz, DMSO-d_6): δ 8.56 (br, s, 3H), 7.74 (s, 1H), 7.31–7.34 (m, 2H), 7.25–7.27 (m, 3H), 7.24 (d, J = 8.4 Hz, 1H), 6.50 (d, J = 8.4 Hz, 1H), 4.35 (s, 3H), 4.18 (dd, J = 3.0 Hz and 10.2 Hz, 1H), 3.97–4.00 (m, 1H), 3.88 (s, 3H), 3.84–3.86 (m, 1H), 3.18 (dd, J = 4.8 Hz and 13.2 Hz, 1H), 3.04–3.08 (m, 1H). HRMS (ESI): m/z for $C_{20}H_{22}ClN_2O_3$ $[M+H]^+$: calculated 373.1313, found 373.1321.

3.5.4.11. (*R*)-Methyl 4-(2-amino-3-phenylpropoxy)-7-chloro-1-methyl-1*H*-indole-2-carboxylate hydrochloride (6k). White solid, yield 81%, mp 228.8–230.6 °C, $[\alpha]_D^{25}$ −92.3° (*c* 1, MeOH), ^{1}H

NMR (600 MHz, DMSO-d_6): δ 8.40 (s, 3H), 7.73 (s, 1H), 7.32–7.34 (m, 2H), 7.24–7.28 (m, 4H), 6.51 (d, J = 8.4 Hz, 1H), 4.35 (s, 3H), 4.17 (dd, J = 2.4 Hz and 10.2 Hz, 1H), 3.96–3.99 (m, 1H), 3.88 (s, 3H), 3.87 (m, 1H), 3.13–3.15 (m, 1H), 3.04–3.08 (m, 1H). HRMS (ESI): m/z for $C_{20}H_{22}ClN_2O_3$ $[M+H]^+$: calculated 373.1313, found 373.1319.

3.5.4.12. (*R*)-Methyl 4-(2-amino-3-(1*H*-indol-3-yl)propoxy)-7-chloro-1-methyl-1*H*-indole-2-carboxylate hydrochloride (6l). White solid, yield 88%, mp 223.2–226.6 °C, $[\alpha]_D^{25}$ −83.3° (c 1, MeOH), ^{1}H NMR (600 MHz, DMSO-d_6): δ 11.03 (s, 1H), 8.45 (s, 3H), 7.76 (s, 1H), 7.60 (d, J = 7.8 Hz, 1H), 7.37 (d, J = 8.4 Hz, 1H), 7.21–7.24 (m, 2H), 7.08 (t, J = 7.2 Hz, 1H), 6.97 (t, J = 7.2 Hz, 1H), 6.48 (d, J = 8.4 Hz, 1H), 4.35 (s, 3H), 4.23 (dd, J = 2.4 Hz and 10.2 Hz, 1H), 4.07 (dd, J = 5.4 Hz and 10.2 Hz, 1H), 3.88 (s, 3H), 3.84 (br, s, 1H), 3.21–3.24 (m, 2H). HRMS (ESI): m/z for $C_{22}H_{23}ClN_3O_3$ $[M+H]^+$: calculated 412.1422, found 412.1430.

3.5.4.13. (*S*)-Methyl 4-(2-amino-3-(1*H*-indol-3-yl)propoxy)-7-chloro-1-methyl-1*H*-indole-2-carboxylate hydrochloride (6m). White solid, yield 80%, mp 223.3–225.9 °C, $[\alpha]_D^{25}$ +64.3° (c 1, MeOH), ^{1}H NMR (600 MHz, DMSO-d_6): δ 11.02 (s, 1H), 8.38 (s, 3H), 7.76 (s, 1H), 7.60 (d, J = 7.8 Hz, 1H), 7.37 (d, J = 7.8 Hz, 1H), 7.23 (d, J = 8.4 Hz, 1H), 7.21 (d, J = 1.8 Hz, 1H), 7.09 (t, J = 7.2 Hz, 1H), 6.97 (t, J = 7.2 Hz, 1H), 6.48 (d, J = 8.4 Hz, 1H), 4.35 (s, 3H), 4.23 (dd, J = 2.4 Hz and 10.2 Hz, 1H), 4.07 (dd, J = 5.4 Hz and 10.2 Hz, 1H), 3.88 (s, 3H), 3.85 (br, s, 1H), 3.18–3.25 (m, 2H). HRMS (ESI): m/z for $C_{22}H_{23}ClN_3O_3$ $[M+H]^+$: calculated 412.1422, found 412.1429.

3.5.4.14. (*S*)-1-((7-Methoxy-1-methyl-2-(3-methyl-1,2,4-oxadiazol-5-yl)-1*H*-indol-4-yl)oxy)-3-phenylpropan-2-amine hydrochloride (6n). White solid, yield 85%, mp 155.5–158.6 °C, $[\alpha]_D^{25}$ +47.1° (c 1, MeOH), ^{1}H NMR (600 MHz, DMSO-d_6): δ 8.43 (s, 3H), 7.82 (s, 1H), 7.32–7.35 (m, 2H), 7.25–7.28 (m, 3H), 6.70 (d, J = 8.4 Hz, 1H), 6.39 (d, J = 8.4 Hz, 1H), 4.39 (s, 3H), 4.12 (dd, J = 2.4 Hz and 10.2 Hz, 1H), 3.93–3.96 (m, 1H), 3.88 (s, 3H), 3.84 (m, 1H), 3.15 (dd, J = 5.4 Hz and 13.2 Hz, 1H), 3.06–3.09 (m, 1H), 2.45 (s, 3H). HRMS (ESI): m/z for $C_{22}H_{25}N_3O_4$ $[M+H]^+$: calculated 393.1921, found 393.1928.

3.5.4.15. (*R*)-1-((7-Methoxy-1-methyl-2-(3-methyl-1,2,4-oxadiazol-5-yl)-1*H*-indol-4-yl)oxy)-3-phenylpropan-2-amine hydrochloride (6o). White solid, yield 80%, mp 155.5–157.9 °C, $[\alpha]_D^{25}$ −58.3° (c 1, MeOH), ^{1}H NMR (600 MHz, DMSO-d_6): δ 8.39 (s, 3H), 7.82 (s, 1H), 7.32–7.35 (m, 2H), 7.26–7.29 (m, 3H), 6.71 (d, J = 7.8 Hz, 1H), 6.39 (d, J = 7.8 Hz, 1H), 4.35 (s, 3H), 4.13 (dd, J = 2.4 Hz and 10.2 Hz, 1H), 3.93–3.96 (m, 1H), 3.88 (s, 3H), 3.84 (m, 1H), 3.14 (dd, J = 5.4 Hz and 13.2 Hz, 1H), 3.06–3.09 (m, 1H), 2.45 (s, 3H). HRMS (ESI): m/z for $C_{22}H_{25}N_3O_4$ $[M+H]^+$: calculated 393.1921, found 393.1928.

3.5.4.16. (*S*)-1-(1*H*-Indol-3-yl)-3-((7-methoxy-1-methyl-2-(3-methyl-1,2,4-oxadiazol-5-yl)-1*H*-indol-4-yl)oxy)propan-2-amine hydrochloride (6p). White solid, yield 84%, mp 169.7–173.9 °C, $[\alpha]_D^{25}$ +30.8° (c 1, MeOH), ^{1}H NMR (600 MHz, DMSO-d_6): δ 11.05 (s, 1H), 8.48 (s, 3H), 7.85 (s, 1H), 7.63 (d, J = 7.8 Hz, 1H), 7.37 (d, J = 8.4 Hz, 1H), 7.23 (s, 1H), 7.09 (t, J = 7.8 Hz, 1H), 6.98 (t, J = 7.8 Hz, 1H), 6.69 (d, J = 8.4 Hz, 1H), 6.37 (d, J = 8.4 Hz, 1H), 4.38 (s, 3H), 4.18 (dd, J = 2.4 Hz and 10.2 Hz, 1H), 4.03–4.05 (m, 1H), 3.87 (s, 3H), 3.83 (m, 1H), 3.21–3.29 (m, 2H), 2.45 (s, 3H). HRMS (ESI): m/z for $C_{24}H_{26}N_5O_3$ $[M+H]^+$: calculated 432.2030, found 432.2038.

3.5.4.17. (*R*)-1-(1*H*-Indol-3-yl)-3-((7-methoxy-1-methyl-2-(3-methyl-1,2,4-oxadiazol-5-yl)-1*H*-indol-4-yl)oxy)propan-2-amine hydrochloride (6q). White solid, yield 92%, mp 169.9–173.5 °C, $[\alpha]_D^{25}$ −46.7° (c 1, MeOH), ^{1}H NMR (600 MHz, DMSO-d_6): δ 11.02 (s, 1H), 8.31 (s, 3H), 7.84 (s, 1H), 7.61 (d, J = 8.4 Hz, 1H), 7.37 (d, J = 8.4 Hz, 1H), 7.23 (d, J = 1.8 Hz, 1H), 7.09 (t, J = 7.8 Hz, 1H), 6.98 (t, J = 7.8 Hz, 1H), 6.70 (d, J = 8.4 Hz, 1H), 6.38 (d, J = 8.4 Hz, 1H), 4.39 (s, 3H), 4.18 (dd, J = 3.0 Hz and 10.2 Hz, 1H), 4.02–4.04 (m, 1H), 3.87 (s, 3H), 3.87 (m, 1H), 3.22 (d, J = 7.8 Hz, 2H), 2.45 (s, 3H). HRMS (ESI): m/z for $C_{24}H_{26}N_5O_3$ $[M+H]^+$: calculated 432.2030, found 432.2038.

3.5.4.18. (*S*)-1-((7-Methoxy-1-methyl-2-(3-methyl-1,2,4-oxadiazol-5-yl)-1*H*-indol-4-yl)oxy)-4-(methylthio)butan-2-amine hydrochloride (6r). White solid, yield 84%, mp 209.4–213.2 °C, $[\alpha]_D^{25}$ +15.4° (c 1, MeOH), ^{1}H NMR (600 MHz, DMSO-d_6): δ 8.17 (s, 3H), 7.77 (s, 1H), 6.76 (d, J = 7.8 Hz, 1H), 6.53 (d, J = 7.8 Hz, 1H), 4.38 (s, 3H), 4.28 (dd, J = 2.4 Hz and 10.2 Hz, 1H), 4.10–4.13 (m, 1H), 3.89 (s, 3H), 3.70 (br, s, 1H), 2.65 (t, J = 7.8 Hz, 2H), 2.45 (s, 3H), 2.08 (s, 3H), 1.99–2.03 (m, 2H). HRMS (ESI): m/z for $C_{18}H_{25}N_4O_3$ $[M+H]^+$: calculated 377.1642, found 377.1648.

3.5.4.19. (*S*)-1-((7-Methoxy-1-methyl-2-(3-methyl-1,2,4-oxadiazol-5-yl)-1*H*-indol-4-yl)oxy)-4-methylpentan-2-amine hydrochloride (6s). White solid, yield 93%, mp 214.3–216.5 °C, $[\alpha]_D^{25}$ +17.6° (c 1, MeOH), ^{1}H NMR (600 MHz, DMSO-d_6): δ 8.22 (s, 3H), 7.78 (s, 1H), 6.75 (d, J = 8.4 Hz, 1H), 6.52 (d, J = 8.4 Hz, 1H), 4.37 (s, 3H), 4.25 (dd, J = 3.0 Hz and 10.2 Hz, 1H), 4.06–4.08 (m, 1H), 3.89 (s, 3H), 3.61 (br, s, 1H), 2.46 (s, 3H), 1.76–1.80 (m, 1H), 1.60–1.62 (m, 2H), 0.94 (d, J = 6.6 Hz, 3H), 0.92 (d, J = 6.6 Hz, 3H). HRMS (ESI): m/z for $C_{19}H_{27}N_4O_3$ $[M+H]^+$: calculated 359.2078, found 359.2084.

Acknowledgments

This work was supported by the National Natural Science Foundation of China (No. 21072115) and Shandong Natural Science Foundation (No. ZR2011HM042). The convenience afforded by the Institute of Immunopharmacology and Immunotherapy in the School of Pharmaceutical Sciences at Shandong University for the biological assays was appreciated.

References and notes

1. Wendel, H. G.; De Stanchina, E.; Fridman, J. S.; Malina, A.; Ray, S.; Kogan, S.; Cordon-Cardo, C.; Pelletier, J.; Lowe, S. W. *Nature* **2004**, *428*, 332.
2. Kallan, N. C.; Spencer, K. L.; Blake, J. F.; Xu, R.; Heizer, J.; Bencsik, J. R.; Mitchell, I. S.; Gloor, S. L.; Martinson, M.; Risom, T., et al *Bioorg. Med. Chem. Lett.* **2011**, *21*, 2410.
3. Cully, M.; You, H.; Levine, A. J.; Mak, T. W. *Nat. Rev. Cancer* **2006**, *6*, 184.
4. Omar, B.; Zmuda-Trzebiatowska, E.; Manganiello, V.; Goransson, O.; Degerman, E. *Cell Signal.* **2009**, *21*, 760.
5. Wang, P.; Zhang, L.; Hao, Q.; Zhao, G. *Mini-Rev. Med. Chem.* **2011**, *11*, 1093.
6. Pal, S. K.; Reckamp, K.; Yu, H.; Figlin, R. A. *Expert Opin. Investig. Drugs* **2010**, *19*, 1355.
7. Al-Bazz, Y. O.; Underwood, J. C.; Brown, B. L.; Dobson, P. R. *Eur. J. Cancer* **2009**, *45*, 694.
8. Shtilbans, V.; Wu, M.; Burstein, D. E. *Ann. Diagn. Pathol.* **2008**, *12*, 153.
9. Datta, S. R.; Dudek, H.; Tao, X.; Masters, S.; Fu, H.; Gotoh, Y.; Greenberg, M. E. *Cell* **1997**, *91*, 231.
10. Ichijo, H.; Nishida, E.; Irie, K.; ten Dijke, P.; Saitoh, M.; Moriguchi, T.; Takagi, M.; Matsumoto, K.; Miyazono, K.; Gotoh, Y. *Science* **1997**, *275*, 90.
11. Pan, J.; Chang, Q.; Wang, X.; Son, Y.; Zhang, Z.; Chen, G.; Luo, J.; Bi, Y.; Chen, F.; Shi, X. *Chem. Res. Toxicol.* **2010**, *23*, 568.
12. Li, J.; Yuan, J. *Oncogene* **2008**, *27*, 6194.
13. Cardone, M. H.; Roy, N.; Stennicke, H. R.; Salvesen, G. S.; Franke, T. F.; Stanbridge, E.; Frisch, S.; Reed, J. C. *Science* **1998**, *282*, 1318.
14. Cantarelli, B.; Duca, L.; Blanchevoye, C.; Poitevin, S.; Martiny, L.; Debelle, L. *FEBS Lett.* **2009**, *583*, 2385.
15. Zheng, T.; Meng, X.; Wang, J.; Chen, X.; Yin, D.; Liang, Y.; Song, X.; Pan, S.; Jiang, H.; Liu, L. *J. Cell. Biochem.* **2010**, *111*, 218.
16. Qu, Y.; Wang, J.; Sim, M. S.; Liu, B.; Giuliano, A.; Barsoum, J.; Cui, X. *Breast Cancer Res. Treat.* **2010**, *121*, 311.
17. Diehl, J. A.; Cheng, M.; Roussel, M. F.; Sherr, C. J. *Genes Dev.* **1998**, *12*, 3499.
18. Wei, W.; Jin, J.; Schlisio, S.; Harper, J. W.; Kaelin, W. G., Jr. *Cancer Cell* **2005**, *8*, 25.

19. Welcker, M.; Singer, J.; Loeb, K. R.; Grim, J.; Bloecher, A.; Gurien-West, M.; Clurman, B. E.; Roberts, J. M. *Mol. Cell* **2003**, *12*, 381.
20. Yeh, E.; Cunningham, M.; Arnold, H.; Chasse, D.; Monteith, T.; Ivaldi, G.; Hahn, W. C.; Stukenberg, P. T.; Shenolikar, S.; Uchida, T., et al *Nat. Cell Biol.* **2004**, *6*, 308.
21. Wang, P.; Liu, J.; Xing, H.; Liu, Y.; Xie, W.; Zhao, G. *Drug Discovery Ther.* **2012**, *6*, 133.
22. Mishra, J. K.; Panda, G. *J. Comb. Chem.* **2007**, *9*, 321.
23. Manivel, P.; Rai, N. P.; Jayashankara, V. P.; Arunachalam, P. N. *Tetrahedron Lett.* **2007**, *48*, 2701.
24. Heerding, D. A.; Rhodes, N.; Leber, J. D.; Clark, T. J.; Keenan, R. M.; Lafrance, L. V.; Li, M.; Safonov, I. G.; Takata, D. T.; Venslavsky, J. W., et al *J. Med. Chem.* **2008**, *51*, 5663.
25. Donald, A.; McHardy, T.; Rowlands, M. G.; Hunter, L.-J. K.; Davies, T. G.; Berdini, V.; Boyle, R. G.; Aherne, G. W.; Garrett, M. D.; Collins, I. *J. Med. Chem.* **2007**, *50*, 2289.
26. Caldwell, J. J.; Davies, T. G.; Donald, A.; McHardy, T.; Rowlands, M. G.; Aherne, G. W.; Hunter, L. K.; Taylor, K.; Ruddle, R.; Raynaud, F. I. *J. Med. Chem.* **2008**, *51*, 2147.